Acta Cryst. (1988). A44, 437–442

Effective Resolution of Macromolecular X-ray Diffraction Data

BY STANLEY M. SWANSON

Biographics Laboratory, Department of Biochemistry and Biophysics, Texas A&M University, College Station, Texas 77843-2128, USA

(*Received* 28 *July* 1987; *accepted* 2 *February* 1988)

Abstract

'Effective resolution' is a practical quantitative measure of the extent, quality, and completeness of X-ray diffraction data. Sparrow's [*Astrophys. J.* (1916), **44**, 76–86] criterion for the separation of just-resolved peaks is applied to a typical electron density peak shape, which, in turn, is the Fourier transform of an average form factor derived from the observed F_{hkl}'s. Numerical studies of a Gaussian form factor, with appropriate modifications for atomic scattering factors, give a quantitative picture of the dependence of resolution on both the amount of data and the underlying structural features. The relation between effective resolution and nominal resolution (d_{min}) depends only on the ratio of the limiting high-resolution peak width to d_{min}.

Introduction

Even good protein data suffer from increasing numbers of weak reflections for d spacings below 2·0 Å. A rapid increase in the percentage of weak and unmeasured reflections from 2·0 to 1·65 Å in an elastase–inhibitor complex studied in this laboratory (Meyer, Radhakrishnan, Cole & Presta, 1986) motivated this inquiry into how one can accurately describe the resolution of such data.

The nominal resolution (d_{min}) indicates the extent of data in reciprocal space, but not its quality or completeness. I propose in this paper an empirical measure of resolution which deals quantitatively with various causes of peak broadening, including randomly distributed unmeasured reflections.

The conventional treatment of resolution is inadequately based on a point-atom model. I present an approximate but quantitative treatment of the variation of resolution as a function of d_{min} when atoms are not points and $B \neq 0$. A single 'universal' resolution curve emerges which depends on a normalized distance. There is an internal scale determined by the quality of the data which indicates whether or not atomic resolution can be obtained.*

* A program listing and commentary has been deposited with the British Library Document Supply Centre as Supplementary Publication No. SUP 44704 (11 pp.). Copies may be obtained through The Executive Secretary, International Union of Crystallography, 5 Abbey Square, Chester CH1 2HU, England.

0108-7673/88/040437-06$03.00

Resolution and peak separation in real space

Resolution deals with how much detail can be seen in an image. In protein crystallography, the image is the electron density map which consists of a sum of blurred image peaks corresponding to the atoms in the structure. The peaks will be broadened beyond the intrinsic size of the electron distribution by thermal motion, disorder and Fraunhofer diffraction effects. In optics it is the Fraunhofer diffraction from a single extended aperture which blurs an image and determines resolving power (Strong, 1958; Born & Wolf, 1965).

The smallest separation at which image peaks are still individually identifiable is a theoretical limit to resolution which I will call the *critical separation*. The analysis can be reduced to a consideration of the sum of two peaks. It is easy to see what happens in the two limiting cases of separation: when the centers of two peaks are coincident, they sum to a single peak

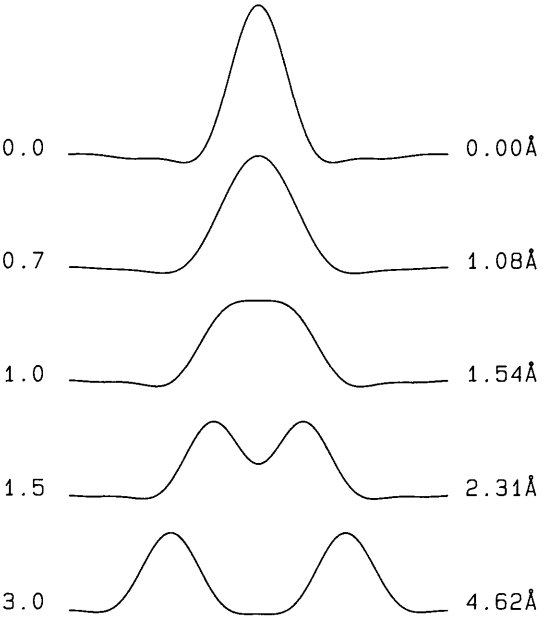

Fig. 1. The sum of two typical density peaks of an elastase–inhibitor complex (a), at various separations. The curves are labeled on the right by the distance between the peak centers, and on the left by the ratio of this distance to the critical separation where a saddle just begins to form (d_{min} = 1·65 Å).

of double height, whereas at large separations one sees essentially two peaks, with slight distortions due to ripples in the tails. The intermediate cases are harder to characterize and depend in detail on peak shape and breadth. The sum of two typical density peaks of an elastase-inhibitor complex is shown in Fig. 1 for several peak separations.

Consider a curve which is symmetrical about a single maximum. The sum of two identical copies of such a curve with their peaks offset will have a local minimum at the midpoint between the individual peak positions when the separation of their central maxima exceeds twice the distance from the maximum to the first inflection point for an individual curve. Two peaks are visible in the sum at separations greater than this critical distance. Note that one matches the inflection points of the two curves rather than superimposing the maximum of one with the first minimum of the other as is customary with the Rayleigh definition of resolution (Strutt, 1879).

The use of the first inflection point of an image peak to define the resolution limit is due to Sparrow (1916). He made some observations on simulated images of optical spectral lines which showed that this limit is actually achievable: two lines at this minimum separation appear as a doublet to the eye. In the past, the 'limit of resolution' has been given in terms of the Rayleigh limit (James, 1948; Stenkamp & Jensen, 1984). The Rayleigh limit for a point atom in three dimensions ($=0{\cdot}917d_{\min}$) is somewhat larger than the minimum separation at which the two peaks can be distinguished ($=0{\cdot}796d_{\min}$) given by the Sparrow limit.

Method

Neither of these ideal limits accurately describes real data. I propose an effective resolution,

$$D_{\text{eff}} = 2{\cdot}5 \times \begin{pmatrix} \text{the distance from the central maximum} \\ \text{to the first radial inflection point} \\ \text{of a typical image peak} \end{pmatrix}, \quad (1)$$

which is to be evaluated for each structure. To be consistent with the present usage of $d_{\min}$ as a measure of resolution, the scale factor is chosen so that D_{eff} equals $d_{\min}$ in the low-resolution limit. (More precisely, the scale factor is 2·511... and is derived from the first inflection point of the image peak for a point atom.) There are two types of distances here: an interplanar spacing symbolized by d and a distance between peak centers given by D. In practice D_{eff} is somewhat larger than the nominal resolution owing to the inclusion of peak-broadening effects, although the omission of very-low-angle data can make it smaller than $d_{\min}$ at low resolution. Since D_{eff} is 1·25 times the Sparrow limit, peaks at this separation will have a saddle between them; this will be discussed in greater detail below.

For the determination of the effective resolution of data, a typical image peak is taken to be the Fourier transform of an average form factor calculated from the measured data. A form factor is a single function which combines the effects of atomic scattering factors and temperature factors. Examples of form factors and their transforms for two experimental structures and two theoretical models are given in Figs. 2 and 3.

To obtain $F_{\text{ave}}(s)$, average the observed F_{hkl}'s in a narrow spherical shell from s to $s+\Delta s$, where

$$s = 1/d = 2(\sin\theta)/\lambda. \quad (2)$$

Sum the magnitudes of the observed F's and divide by the number of all reciprocal-lattice points in the shell, counting unmeasured and space-group-extinct reflections as well as the measured reflections. If data

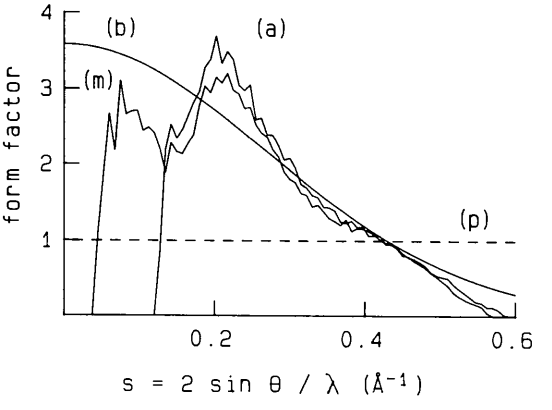

Fig. 2. Average form (scattering) factors for two empirical, (*m*), (*a*), and two theoretical cases, (*p*), (*b*). The relative normalizations are consistent with unit peak height in Fig. 3: (*p*) point atom, $B = 0$, calculated; (*b*) point atom, $B = 25$ Å^2, calculated; (*a*) elastase with inhibitor, observed; (*m*) native elastase, observed.

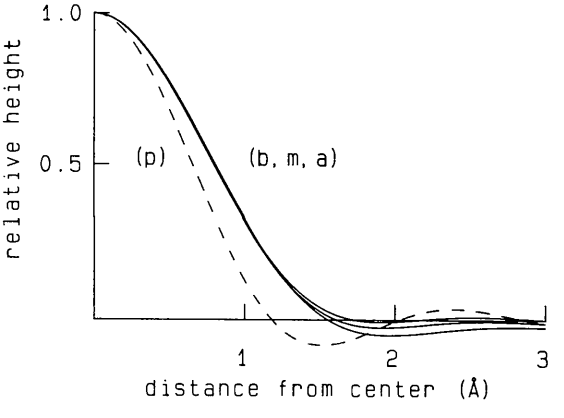

Fig. 3. A selection of image peaks at $d_{\min} = 1{\cdot}65$ Å, corresponding to the form factors given in Fig. 2. Peak height is normalized to 1 so that differences in width are readily apparent. Curves (*b*), (*a*) and (*m*) are almost identical from the central maximum to well past the first inflection point.

are restricted to less than a sphere by the symmetry group, suitable weights should be used to compensate for multiple counting on boundaries.

The procedure is reminiscent of a Wilson plot, but yields an estimate of the form factor directly instead of parametrizing it in terms of an average atomic scattering factor and an overall temperature factor. It includes the effects of temperature and disorder fall-off, and reduces the scattering power in shells where there are many unmeasured reflections. In addition, $F_{ave}(s)$ is zero where there are no data. If the density map is determined from part of the data, or if the high-angle F's have been modified to smooth or sharpen the map, it is this restricted or modified set of F's which should be used to calculate $F_{ave}(s)$.

This average form factor transforms to a spherically symmetric density $\rho(r)$. The numerical calculation of ρ can be simplified by using a pseudocell in which $a=b=c$ and $\alpha=\beta=\gamma=90°$. By choosing r along the x axis, the triple sum can be written as

$$\rho(x) \propto \sum_{h=0}^{m} F_h \cos 2\pi hx, \qquad (3)$$

where

$$F_h = \sum_{k=0}^{m} \sum_{l=0}^{m} w_{hkl} F_{ave}(s_{hkl}). \qquad (4)$$

The weights w_{hkl} compensate for double counting on the faces, edges and apex of the octant (one, two or three indices equal zero: $w=4$, 2, 1 respectively) as compared with the interior ($w=8$). The restriction

$$s_{hkl}^2 = (h^2+k^2+l^2)/a^2 \le m^2/a^2 \simeq s_{max}^2 \qquad (5)$$

is implicit in $F_{ave}(s)$. The resulting sum is easily evaluated (for some of the examples in this paper, $a=60$ Å; in others, $a=40d_{min}$). To find the effective resolution, the first zero of the second derivative of ρ is needed; this can be found from the F_h's as

$$\rho''(x) \propto -\sum_{h=0}^{m} h^2 F_h \cos 2\pi hx. \qquad (6)$$

Examples

Effective resolution has been determined for a native porcine pancreatic elastase structure (Meyer, Cole, Radhakrishnan & Epp, 1988) denoted by (m), and for three elastase–inhibitor complexes: that of Meyer *et al.* (1986), denoted by (a), and two of Radhakrishnan, Presta, Meyer & Wildonger (1987), denoted by (c) and (z). Data sets were taken on film in three cases (m, a, c) and with an area detector in the other (z). All data sets have poor percent-observed figures in the last few shells, owing partly to systematic exclusions of data in certain directions due to collection geometry, so that the nominal resolution is not really a fair measure of the extent of the data.

Table 1. *Effective resolution of four elastase structures*

Increasing amounts of the observed data ($d > d_{cut}$) were used to calculate D_{eff} for a native elastase structure (m), and three inhibited structures (a), (c), (z). The corresponding d_{min}'s are 1·65, 1·65, 1·76 and 2·09 Å.

	D_{eff}			
d_{cut}	(m)	(a)	(c)	(z)
2·5	2·62	2·61	2·61	2·63
2·4	2·53	2·53	2·52	2·53
2·3	2·43	2·43	2·42	2·44
2·2	2·33	2·33	2·33	2·34
2·1	2·23	2·24	2·24	2·25
2·0	2·14	2·15	2·15	
1·9	2·05	2·06	2·06	
1·8	1·97	1·99	1·98	
1·7	1·91	1·94	1·94	
1·6	1·87	1·93		

Table 2. *A consistency check*

The average form factor was determined from calculated F_{hkl}'s using protein coordinates with $B=15$ Å^2 and all atoms assumed to be carbon.

s	$f(s)$	$F_{C\,ave}(s)$
0·1	5·54	5·43
0·2	4·38	5·06
0·3	3·08	3·08
0·4	1·95	1·62
0·5	1·16	1·04
0·6	0·65	0·53

In Table 1, effective resolution is tabulated for successively larger fractions of the data from these four elastase structures. The numbers agree until a few tenths of an ångström from the limit of data collection for any given structure. This suggests that the limitation on resolution here is the amount of data collected, rather than variations in crystal quality. The theoretical analysis in the next section indicates that resolution is still (Fraunhofer) diffraction limited at $d_{min} > 1·8$ Å.

Does F_{ave} actually capture the characteristics of the underlying atomic form factors? As a consistency check on the method, a numerical test was performed. If one starts with a known atomic scattering factor and a known temperature factor, does the evaluation of F_{ave} from calculated structure factors recover the initial form factor,

$$f(s) = f_{atomic}(s) \exp(-Bs^2/4)? \qquad (7)$$

The test was made with a set of refined coordinates for the non-hydrogen atoms of elastase, with all atoms being given a B of 15 Å^2 and scattering factors for carbon. The results, in Table 2, are encouraging. In the range $0·1 < s < 0·6$ Å^{-1}, the agreement is 13% r.m.s. after scaling by a constant factor. The fall-off of F_{ave} with increasing s is the same or perhaps a little more rapid than $f(s)$. A modest rise of F_{ave} is seen near 5 Å, which is characteristic of protein structures.

Universal resolution curves

As the nominal resolution varies, the apparent size of atoms changes. The interplay between the effects of the amount of data available and the intrinsic size of the atoms is described by a simple curve. At very low resolution the size is proportional to d_{min}, while in the high-resolution limit it approaches a constant. A model based on a Gaussian form factor,

$$f(s) = \exp(-\mathcal{B}s^2/4), \tag{8}$$

illustrates the changing importance of the two effects. $\mathcal{B}$ is written instead of B to emphasize that more than just thermal motion is included in the model. In the limit $d_{min} = 0$, the Fourier transform of this form factor is also a Gaussian, with standard deviation $(\mathcal{B}/2)^{1/2}/2\pi$ (variance $\mathcal{B}/8\pi^2$). The critical separation for two Gaussian peaks is twice the standard deviation, which I will take as the measure of the intrinsic width of the peak,

$$W = (\mathcal{B}/2)^{1/2}/\pi. \tag{9}$$

It is perhaps more appropriate to think of resolution in terms of s_{max} than d_{min} because high resolution corresponds to large values of the inverse distance. Just as one thinks of distances from the mean of a Gaussian distribution in terms of multiples of the standard deviation, the distances in this model can be normalized to the limiting critical distance W,

$$t = W/d_{min} = Ws_{max}. \tag{10}$$

Peak center separations, D, corresponding to different amounts of saddle were determined numerically for a range of ε, $\mathcal{B}$ and S_{max} in this Gaussian model. The parameter

$$\varepsilon = (\text{peak} - \text{saddle})/(\text{peak}) \tag{11}$$

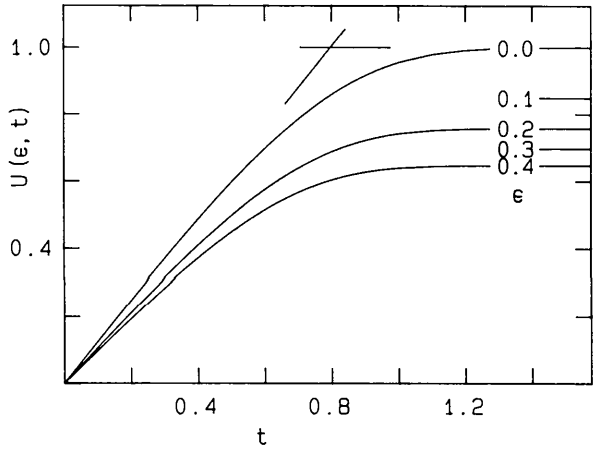

Fig. 4. The normalized reciprocal separation $U(\varepsilon, t)$ as a function of the normalized reciprocal nominal resolution $t = (\mathcal{B}/2)^{1/2}s_{max}/\pi$. Curves are given for saddle dips $\varepsilon = 0$, 0·2, 0·4, and the horizontal asymptotes indicated for intermediate values. The intersection of the initial slope and final asymptote is shown for $\varepsilon = 0$.

denotes the dip at the midpont saddle relative to the peak maxima in the density sum curve. Instead of requiring separate curves $D(\varepsilon, \mathcal{B}, s_{max})$ for each ε and $\mathcal{B}$, the results are concisely expressible in terms of a normalized reciprocal separation, U:

$$D(\varepsilon, t) = W/U(\varepsilon, t) = 1/S(\varepsilon, t). \tag{12}$$

The asymptotic value $U(0, \infty)$ is 1, corresponding to $D(0, \infty) = 0{\cdot}225\mathcal{B}^{1/2}$. Since $U_{eff}(t) = 0{\cdot}7965\,U(0, t)$,

$$D_{eff}(\infty) = 0{\cdot}282\mathcal{B}^{1/2}. \tag{13}$$

Qualitatively, Fig. 4 shows two limits: low resolution where the effective resolution is nearly proportional to the nominal resolution, and extremely high resolution where the effective resolution is almost constant. The transition region between the limiting cases occurs when t is near unity and corresponds approximately to the domain of high-resolution protein crystallography ($2 > d_{min} > 1$ Å, for overall B's about 15 Å^2).

So long as a curve remains near the initial slope, resolution is (Fraunhofer) diffraction limited, determined more by the amount of data than by the underlying characteristics of the atoms. Conversely, when a curve nears its final constant value, the structure, motion and disorder of the scatterers dominates; taking additional data (assuming one can measure it) will not much reduce the apparent size of the atoms. Nowhere does the effective resolution depart more than 20% from one or other of the limiting lines.

Not only can one scale out the effect of different $\mathcal{B}$, but each of the curves for different ε in Fig. 4 has almost the same shape aside from vertical and horizontal scaling. The shape is approximated by

$$\tau(1 + \tau^2 + \tau^8)^{-1/8} \tag{14}$$

to better than 3%. The horizontal scale is the crossover point, $t_x(\varepsilon)$, the abscissa of the point where the extrapolation of the initial slope equals the final constant value $U(\varepsilon, \infty)$, so that

$$\tau = t/t_x(\varepsilon). \tag{15}$$

If the function

$$g(\tau, \varepsilon) = U[\varepsilon, \tau t_x(\varepsilon)]/U(\varepsilon, \infty) \tag{16}$$

is plotted for the values of ε given in Table 3, the curves lie on top of each other initially and asymptotically. The worst agreement is at the crossover point where the values range from 0·807 to 0·857, with a mean of 0·842 and a r.m.s. discrepancy of 0·014. Values for scaling are given in Table 3, as well as the value of $U[\varepsilon, t_x(\varepsilon)]$ at the crossover point.

The case $\varepsilon = 0$ gives the critical separation or Sparrow limit of resolution, $D(0, t)$. Because of the utility of this curve after various scaling transformations, an accurate numerical fit has been determined. The

Table 3. *Parameters for universal curves*

Dip ε	Initial slope $U_i(\varepsilon, 0)$	Final value $U(\varepsilon, \infty)$	Crossover value $U[\varepsilon, t_x(\varepsilon)]$	Crossover position $t_x(\varepsilon)$
0·00	1·255	1·000	0·857	0·796
0·05	1·212	0·930	0·750	0·767
0·10	1·138	0·848	0·709	0·746
0·15	1·099	0·797	0·673	0·725
0·20	1·072	0·758	0·642	0·707
0·25	1·049	0·726	0·614	0·692
0·30	1·026	0·697	0·590	0·679
0·35	1·005	0·671	0·567	0·668
0·40	0·983	0·647	0·546	0·659

reciprocal critical separation curve is

$$U(0, t) = t/(0{\cdot}7966 + 0{\cdot}1380t^2 + 0{\cdot}1134t^4), \quad (17)$$

which has absolute error less than 0·0003 for $t < 0{\cdot}97$. Expression (14) is a better approximation than equation (17) for $t > 1{\cdot}1$, with an error less than 0·7%.

To test the effect of atomic scattering factors, which are not Gaussian, calculations were made with a mean atomic scattering factor, f_{mean}, for an 'average' protein

$$C_{1000}N_{270}O_{370}H_{1680}S_{14}.$$

Curves are shown in Fig. 5 for overall $B = 5$, 15 and 25 Å^2 in the range $0 \le s_{max} \le 1$ Å^{-1}.

The calculation of effective resolution depends predominantly on the shape of F_{ave} near s_{max}. A study of Figs. 2 and 3 shows that large differences in the form-factor curves (b, m, a) for $s < 0{\cdot}1$ Å^{-1} result in only a slight modification of the depth of the first minimum of the image peak and in almost no change in the shape of the peaks closer to the central maximum. Since the dominant contribution to resolution comes from the form factor near s_{max}, the results shown in Fig. 5 can be approximated from $U(0, t)$ by setting

$$\mathcal{B} = B + (4/s_{max}^2) \log [f_{mean}(0)/f_{mean}(s_{max})]. \quad (18)$$

$S(0, B, s_{max})$ is reproduced with relative error less than 2%.

This simple Gaussian model explains the qualitative features of resolution and is effective quantitatively. Although measurement thresholds may cut off F_{ave} more quickly for real data than in the model, the similarity of the typical density peaks in Fig. 3 argues for its applicability, as does the success of the numerical approximation for $\mathcal{B}$. However, the best guide to the resolution of a specific structure is still the typical $\rho(r)$ obtained as the transform of $F_{ave}(s)$.

Comparison of definitions of resolution

Effective resolution is compared with several different formulations of the Rayleigh resolution criterion in Fig. 6. The Rayleigh criterion appears in its original definition as the distance $D_R(t)$ between the central maximum and the first minimum of an image peak, as a linear extrapolation of the point-atom separation

$$D_L = 0{\cdot}917 d_{min}, \quad (19)$$

and as a dip criterion ($\varepsilon = 0{\cdot}19$) applied to arbitrary peaks. When $\mathcal{B} \neq 0$ these definitions are no longer equivalent and all but the last have serious problems as t approaches 0·8.

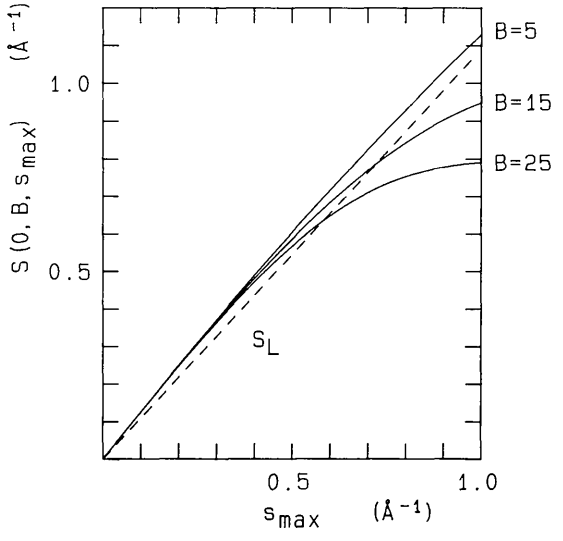

Fig. 5. Reciprocal critical separation $S(0, B, s_{max})$ as a function of reciprocal nominal resolution s_{max}, calculated for a mean atomic scattering factor characteristic of proteins with additional overall $B = 5$, 15 and 25 Å^2. The dotted straight line from the origin gives the Rayleigh resolution for the point-atom case (p).

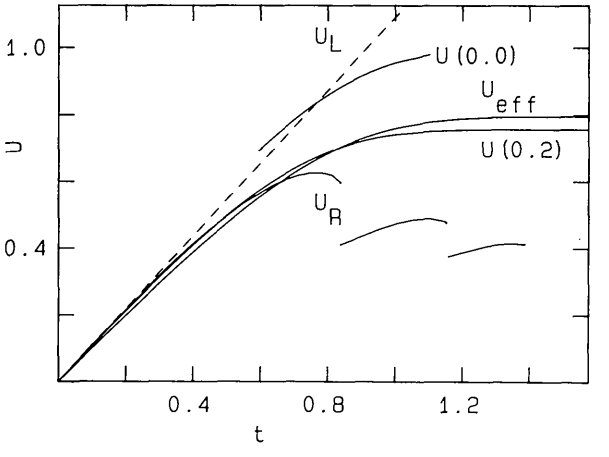

Fig. 6. Comparison of normalized reciprocal effective resolution $U_{eff}(t)$ with $U(0{\cdot}2, t)$ and with several versions of Rayleigh resolution. U_L is the extrapolation of the point atom, $\mathcal{B} = 0$, Rayleigh criterion: note that beyond the crossing at $U(0, 0{\cdot}79)$ only a single peak appears. $U_R(t)$ is the Rayleigh first-minimum criterion applied to $\mathcal{B}$-broadened peaks. The discontinuity at $t = 0{\cdot}837$ occurs when the 'first' minimum disappears; that at $t = 1{\cdot}152$ when the 'second' minimum also disappears.

The curve for $U_{\text{eff}}(t)$ lies close to that for $U(0{\cdot}2, t)$, as seen in Fig. 6. This is also where one would expect the reciprocal separation, $U_R(t)$, based on the observation that point atoms at the Rayleigh separation have $\varepsilon = 0{\cdot}19$. In fact, the first minimum in the peak decreases in depth as $\mathbb{B}$ increases and moves outwards faster than the first inflection point. At $t = 0{\cdot}837$, this 'first' minimum disappears and its role is taken by what was the second minimum, giving a discontinuity in $U_R(t)$. Even before this, at $t = 0{\cdot}63$, the separation and hence ε determined by the Rayleigh criterion has exceeded that for $U(0{\cdot}2, t)$.

Because $U(\varepsilon, t)$ becomes constant for large t, resolution limits which are proportional to d_{min} will ultimately be wrong. Such limits describe data-limited rather than structure-limited resolution. The simple extrapolation of the point-atom Rayleigh limit suggested by Stenkamp & Jensen (1984), expressed in terms of U,

$$U_L = t/0{\cdot}917, \tag{20}$$

crosses $U(0, t)$ at $t = 0{\cdot}79$, thus no longer producing a saddle between peaks. Their example (nitrogen, $B = 10$ Å^2, $s_{\text{max}} = 0{\cdot}5$ Å^{-1}) is still data limited, corresponding to $t = 0{\cdot}50$. When compared with the $S(0, B, s_{\text{max}})$ curves in Fig. 5,

$$S_L = s_{\text{max}}/0{\cdot}917 \tag{21}$$

does lie below the $B = 5$ Å^2 curve all the way to $s_{\text{max}} = 1$, but crosses the $B = 15$ Å^2 curve at $s_{\text{max}} = 0{\cdot}68$.

Further applications

Effective resolution was designed to measure the quality and completeness of data on a case-by-case basis. Once the machinery to calculate typical density peaks is in place, other questions can be answered. For example, an easy calculation will tell whether holes can be seen in six- or five-membered rings for specific data. When should data collection stop? Are the data in the outer shells good enough to justify the effort in collecting more or refining them? Will more data of the current quality add any significant resolution to the study?

When the critical separation is known for given data, one knows the minimum distance between identifiable atoms in the absence of noise. With some idea of the noise spectrum, the information about the separation required for a certain size of saddle could provide a probability that apparent features are real rather than just random fluctuations in ridges. Some guidance about the choice of a contouring threshold for electron density may be forthcoming.

There is interest in effective resolution as a measure of quality for protein crystals grown in space (Bugg, 1987). The method gives a single quantitative measure of the extent of data in reciprocal space, answering the question: 'How far out does the crystal diffract?' It depends on the average diffraction amplitude in a resolution shell, whereas a percent-observed figure depends on an experimental threshold of observability. It is not yet known how sensitive effective resolution would be as a measure of crystal quality. Quick reliable estimates of $F_{\text{ave}}(s)$ would be needed for survey work. In evaluating different crystallization conditions for the same protein, one might be able to use the relative decrease of F_{ave} at a fixed s_{max} rather than measuring out to essentially zero diffracting power.

This work has benefited from continuing discussions with Rosemarie Swanson and from critical readings by R. E. Rosenfield, E. F. Meyer, A. Karrer, and two referees. Financial support has come from the National Science Foundation and the Office of Naval Research.

References

BORN, M. & WOLF, E. (1965). *Principles of Optics*, 3rd ed., pp. 392-418. Oxford: Pergamon Press.

BUGG, C. E. (1987). Private communication.

JAMES, R. W. (1948). *Acta Cryst.* **1**, 132-134.

MEYER, E., COLE, G., RADHAKRISHNAN, R. & EPP, O. (1988). *Acta Cryst.* **B44**, 26-38.

MEYER, E. F. JR, RADHAKRISHNAN, R., COLE, G. M. & PRESTA, L. G. (1986). *J. Mol. Biol.* **189**, 533-539.

RADHAKRISHNAN, R., PRESTA, L. G., MEYER, E. F. JR & WILDONGER, R. (1987). *J. Mol. Biol.* **198**, 417-424.

SPARROW, C. M. (1916). *Astrophys. J.* **44**, 76-86.

STENKAMP, R. E. & JENSEN, L. H. (1984). *Acta Cryst.* **A40**, 251-254.

STRONG, J. (1958). *Concepts of Classical Optics*, pp. 201-212. San Francisco: W. H. Freeman.

STRUTT, J. W. (3RD BARON RAYLEIGH) (1879). *Philos. Mag. Ser.* 5, **8**, 261-274.